Solar-grade boron emitters by BF_3 plasma doping and role of the co-implanted fluorine

Adeline Lanterne, Jerome Le Perchec, Marianne Coig, Frederic Milesi, Julie Boucher, Yannick Veschetti

RESEARCH ARTICLE

Solar-grade boron emitters by BF$_3$ plasma doping and role of the co-implanted fluorine

Adeline Lanterne[1], Jérôme Le Perchec[1]*, Marianne Coig[2], Frédéric Milési[2], Julie Boucher[1] and Yannick Veschetti[1]

[1] CEA, LITEN, INES, 50 avenue du Lac Léman, 73377 Le-Bourget-du-Lac, France
[2] CEA, LETI, Minatec Campus, 17 avenue des Martyrs, 38054 Grenoble, France

ABSTRACT

We investigate the electrical properties and dopant profiles of boron emitters performed by plasma immersion ion implantation from boron trifluoride (BF$_3$) gas precursor, thermally annealed and passivated by silicon oxide/silicon nitride stacks. High thermal budgets are required for doses compatible with screen-printed metal pastes, to reach very good activation rates. However, if good sheet resistances and saturation current densities may be obtained, we met strong limitations of the implied open-circuit voltage of the n-type Czochralski silicon substrates, which is incompatible with high-efficiency solar cells. Such limitations are not encountered with beamline where pure B$^+$ ions are implanted. Efforts on the passivation quality may improve the implied open-circuit voltage but are not sufficient. We provide experimental comparison between beamline and plasma immersion allowing us to discriminate the causes explaining this observation (implantation technique or ion specie used) and to infer our interpretation: The co-implantation of fluorine seems to indirectly impact the lifetime of the core substrate after thermal annealing. Copyright © 2015 John Wiley & Sons, Ltd.

*Correspondence

Le Perchec, Jérôme, CEA, LITEN, Ines, 50 avenue du Lac Leman, 73377 Le-Bourget-du-Lac, France.
E-mail: jerome.le-perchec@cea.fr

## 1. INTRODUCTION: BORON DOPING BY BLII AND PIII

Ion implantation is becoming a more and more used technique to make the photovoltaic (PV) junction of silicon solar cells. It, indeed, offers significant manufacturing simplifications compared with gaseous diffusion-based processes, especially for advanced cells like n-type bifacial or interdigitated back-contact components, and gives highly reproducible and uniform doping, hence tight cell efficiency distributions. Efforts were recently done to reduce the costs of ion implanters dedicated to the solar field, and different kinds of industrial equipment are nowadays present on the market PV [1]: beamline (BLII), ion shower-like, and plasma immersion (PIII) tools. The latter tool is potentially the cheapest one (taking into account running costs) as it is a non mass-selective, surface-independent, low gas consuming implantation equipment. High-quality phosphorous PIII emitters have been largely validated these last years, leading

to conversion efficiencies quite above 19% on p-type industrial size silicon cells with aluminum back surface field [2,3]. Besides, plasma immersion could also serve as a texturization method (black silicon) compatible with the conformal doping of surfaces showing high aspect ratios [4,5].

However, up to now, there are few thorough works showing the use of plasma doping to make solar-grade boron emitters for silicon cells (showing both low emitter saturation current density J_{0e} and high voltage), by resorting to boron trifluoride (BF$_3$) or B$_2$H$_6$ gas precursors for instance. The BLII case has been much more studied and is now well controlled. It is established that boron (B) emitters need high thermal activation annealing to reach low J_{0e} value and may require additional chemical surface treatments to remove the boron-rich layer formed at the surface. Efficiencies around 20.5% have been obtained on large-area n-type homojunction cells [6–9], but to our knowledge, such performances have not been demonstrated with plasma doping (PIII) yet. As a non mass-selective technique, PIII does

not implant pure boron ions but composite ion species depending on the gas precursor we choose ($BF_{x<3}^+$, B^+, F^+ ions with BF_3, $B_2H_{x<6}^+$, B^+, BH_x^+ with B_2H_6). An advantage is that, even for beamline tools, one can obtain much higher ionic current with BF_2^+ ions (for instance) than with pure B^+ ones so that higher throughput implanters devoted to boron doping could be integrated in a solar cell fabrication line. However, the composite ion species can change the physico-chemical behavior of the doping and may complicate the process engineering. In somewhat old publications, Wood *et al.* managed to make efficient n-type cells based on glow-discharge implantation from B_2H_6, either thermally annealed [10] or processed by excimer laser [11], the latter technique giving better results. Recently, B emitters performed on ion shower tool [12] (i.e. without mass selection), and thermally activated, seem to reach sufficient emitter quality (implied V_{oc} of 670 mV), with alumina passivation and an additional forming gas anneal, but information on the actual ion specie implanted is not given and no complete cells were made. Nakamura *et al.* made passivated emitter rear totally diffused (bifacial) solar cells with an ion shower tool [13] and reported efficiencies around 18.5%, limited by recombination losses in the boron emitter. As B_2H_6 is a more toxic, expensive, and unstable gas than BF_3, we will focus on the latter gas in this paper.

Boron doping by BF_3 plasma immersion may present behaviors quite difficult to analyze as we also implant fluorine. Actually, the influence of F on the B activation and diffusion mechanisms is a subject of controversy. Indeed, it is known that BF_2^+ constitutes the majority of implanted specie through the PIII technique [14–16]. Such ions amorphize the silicon surface and may induce end-of-range (EOR) damage such as dislocation loops (DLs) at the initial amorphous/crystalline interface after thermal annealing [17]. Fluorine bubbles may also be trapped in some cases [18]. However, according to other works, fluorine may inhibit (or may dissolve) the formation of EOR DL, by reducing available silicon interstitials [19,20]. Moreover, a chemical fluorine–boron interaction may cause a boron diffusion retardation [21,22], while boron exodiffusion would also be enhanced in the presence of fluorine [23]. Figure 1 shows typical as-implanted boron profiles resulting from beamline and plasma doping. As we can see, these profiles are very different, but the fact that we obtain more concentrated as-implanted profiles with BF_3 plasma doping does not mean that it will be more difficult to activate the dopants because there is an amorphized silicon layer which is reported to be favorable to activation during epitaxial recrystallization and because fluorine may reduce the formation of boron clusters [24]. Indeed, B clusters are responsible for the main limitation of the electrical quality of B^+ implanted emitters, whereas they do not appear in gas diffusion processes [25]. Such boron clusters need high temperatures (typically around 1050 °C) to be dissolved, and if lower temperatures can work with weak implantation doses [7,26], such doses may not be suitable for screen-printing contacts in a solar cell fabrication process. Very recently, Krugener *et al.*
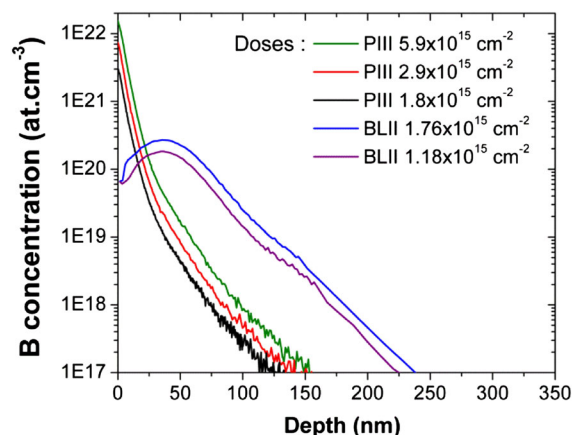

Figure 1. As-implanted boron SIMS profiles after beamline (BLII) and plasma immersion (PIII) ion implantation, for different arbitrary doses and same energy. BLII injects monoenergetic ions and classically gives gaussian-type profiles; the depth of the concentration peak directly depends on the implantation energy. In a plasma chamber, the substrate is immersed in an ionic bath where many collisions occur and the implantation is said to be multienergetic; as a consequence, the dopant profile is shallower and exhibits a maximum at the surface level [3].

[27] presented characterizations of BF_x-based emitters, performed by BLII with different implantation energies and annealing temperatures. They analyzed the silicon crystal damage (via electron microscopy) resulting from BF_x implants and found a process window giving low J_{0e} values (down to 60 fA/cm^2, for a 140 Ω/sq sheet resistance) after a 950 °C annealing and an Al_2O_3 passivation. However, no information was given on implied V_{oc} although it has a strong importance for solar cell integration, as we will see later.

Thus, this paper aims to present a comprehensive (electrical and physicochemical) study enabling the identification of different issues we can meet when we want to make solar-grade boron emitters based on BF_3 plasma doping, followed by a thermal activation, on n-type Czochralski (Cz) 239-cm^2 wafers. In the present work, no cells have been made and we only focus on characterization of symmetrically implanted substrates. After a brief description of the applied process flow, we point out the effects of main plasma parameters and evaluate the boron activation rate after high thermal annealings. Then, we refine our implantation/annealing conditions and highlight the existence of some systematic limitations of emitter electrical parameters that are supposed mainly are supposed to be mainly due to the co-implantation of fluorine. In the second part of the paper, we switch on a beamline tool to check some hypotheses with selectively implanted ions, validating the strong impact of fluorine on the minority carrier lifetime of the silicon substrates.

2. EXPERIMENTAL PROTOCOL

Figure 2 shows the process flow applied on symmetrically implanted n-type Cz wafers. Substrates were chemically
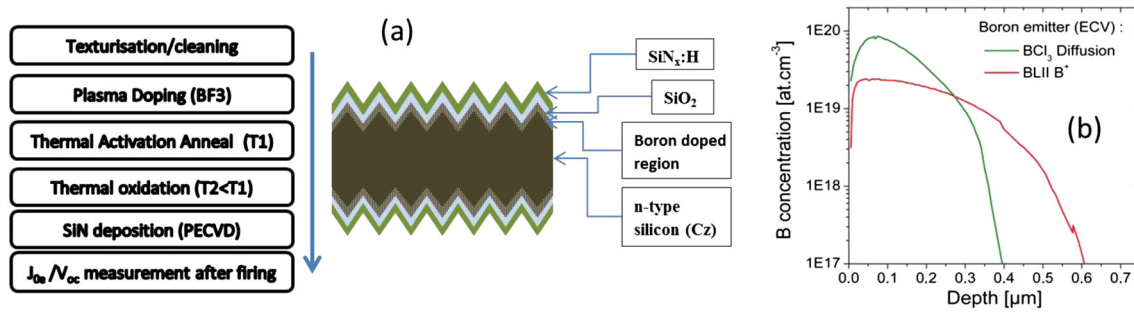
Figure 2. (a) Sketch of the symmetrically implanted samples and process flow (Tx referring to a temperature plateau). (b) Boron electrochemical capacitance-voltage (ECV) profiles of our reference BLII emitter after thermal activation (R_{sheet} = 90 Ω/sq) and that of our BCl_3-diffused emitter (R_{sheet} = 65 Ω/sq) for comparison.

textured by default, but some polished wafers were also used when secondary ion mass spectroscopy (SIMS) measurements were carried out to support our interpretations. For the sake of equivalence, the effective dose implanted on textured wafers must be nearly 1.7 times greater than that on polished ones because of an increased surface area in the presence of pyramids (made by classical KOH texturization).

To electrically activate the dopants, the substrates are submitted to a thermal annealing under neutral (N_2) atmosphere at high temperature, followed by a surface oxidation step at a lower temperature. The surface passivation quality is indeed important, and a silicon oxide growth may be an advantageous method for a solar cell fabrication process as it can be done during the thermal annealing (compared with a separated Al_2O_3 deposition step).

Implantations were all performed at CEA-Leti, either on a Pulsion® plasma immersion equipment (from the company Ion Beam Services), or on a Viista® HC ion beam implanter (from Applied Materials). Cleaning, thermal annealing, passivation steps, and electrical characterizations of the implanted substrates were carried out on the semi-industrial INES platform by CEA-Liten teams. In particular, the implied V_{oc} and the saturation current density J_{0e} were measured by quasi-steady-state photoconductance (QSS-PC) after an infrared firing step. The emitter sheet resistance will be noted R_{sheet}. Regarding PV specifications, our electrical targets are

- $70 < R_{sheet} < 100$ Ω/sq (compatible with good screen-printed contacts)
- $J_{0e} < 200$ fA/cm^2
- Implied $V_{oc} > 650$ mV (>660 mV preferred).

Such targets are related to our standard ion-beam-implanted boron (B^+) emitter which will be taken as a reference all along the paper (refer to its electrochemical capacitance-voltage (ECV) profile in Figure 2 along with a BCl_3 high temperature gaseous diffusion emitter profile for comparison). This BLII reference emitter has indeed been integrated into the fabrication of our high-efficiency bifacial solar devices (up to 20.3% independently certified on 239 cm^2 Cz silicon substrates) called *SONIA* cells [7]. It is

typically characterized by R_{sheet} ~90 Ω/sq, J_{0e} ~150 fA/cm^2, and implied V_{oc} ~660 mV after a 1050 °C thermal activation and a SiO_2 passivation.

3. PLASMA PARAMETERS AND BORON ACTIVATION RATE

First of all, pulsed-plasma conditions were tuned to identify a starting window of implantation dose/emitter sheet resistance suited for PV specifications. Figure 3 gives typical trends of R_{sheet} depending on some variable parameters (radiofrequency (RF) power and gas pressure in the chamber) used on the PIII equipment, for fixed nominal implanted dose and implantation energy, and after a standard 1050 °C thermal annealing (typically applied for beamline boron emitters). RF power and pressure have a strong impact on the BF_3 decomposition in different ionic species [14–16]. The global implanted ionic quantity (machine dose) being fixed here, the observed decrease of R_{sheet} with lower plasma pressure corresponds to greater effective boron doses (implanted and activated dose). In
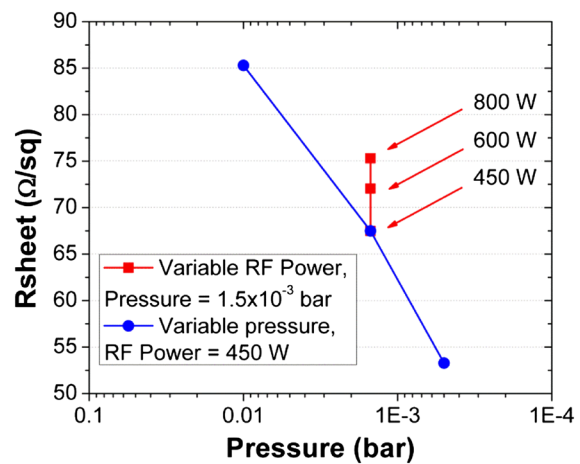
Figure 3. Behavior of the sheet resistance of a boron emitter performed by BF_3 plasma immersion, for fixed machine dose (1×10^{16} at/cm^2) and implantation energy, in function of the radiofrequency power and chamber pressure.

the following, we take a pressure between 5×10^{-4} and 10^{-3} bars and a RF power below 600 W.

It is to be noted that we cannot measure *in situ* the exact dose of boron atoms that we really implant on the plasma tool; contrary to beamline equipment, only the total implanted ionic dose is measured; moreover, a significant amount of superficial implanted boron may exodiffuse or be removed during the whole process. Thus, we experimentally observed that, given our plasma conditions, the real implanted dose is roughly half that of the nominal machine dose.

Efforts (not shown) were also done to adjust the loading and annealing conditions in the belt furnace (temperature ramp-up, N_2 gas flow, time…), in order to minimize the emitter nonuniformity of the 239-cm^2 (textured) silicon wafers. In particular, the BF_3 implants by plasma immersion show a strong concentration at the surface (Figure 1) and are more sensitive to inhomogeneity of the thermal environment than B^+ implants (whose concentration peak is a few nanometers under the surface). All along the paper, we verified that the nonuniformity factors of R_{sheet}, defined according to the ratio

$$Non - unif\,(\%) = 100 \;\; x \left[\frac{R_{sheet\;max} - R_{sheet\;min}}{R_{sheet\;max} + R_{sheet\;min}} \right]$$

were always below 3–4% after a mapping of at least 25 points (such a ratio is a more demanding constraint than the simple standard deviation σ).

We now obtain a first insight into the influence of the thermal annealing on the boron activation. We compare ECV and SIMS profiles of quite heavily doped emitters. As the ECV profile exhibits the activated concentration of dopants while the SIMS profile shows the total concentration of boron, the comparison allows us to calculate the boron activation rate (γ). For that, we use polished Cz silicon wafers. They were implanted with a "machine" dose of 2.9×10^{16} at/cm^2, equivalent to an implantation dose $2.9 \times 10^{16} \times 1.7 = 5 \times 10^{16}$ at/cm^2 on textured surfaces. The substrates were then annealed at two different temperatures

(followed by an oxidation step): one at 950 °C (giving $R_{sheet} = 137\,\Omega/sq$) and the other at 1050 °C with a shorter time ($R_{sheet} = 27\,\Omega/sq$). The curves are displayed in Figure 4.

We see, for each case, a difference between ECV and SIMS measurements that reflects the amount of inactive boron, very close to the surface. Taking into account the uncertainty linked to the sharp B peak at the Si/SiO_2 interface on SIMS profiles, which is only an artifact of the measurement, the activation rate of boron (γ) is between 44 and 58% for the 950 °C annealing whereas it is between 89 and 93% for the very high temperature case. So, we conclude that the activation level is indeed more than adequate, provided that the thermal budget is sufficiently high. Our standard B emitter obtained by beamline implantation corresponds to $\gamma \approx 98\%$ at 1050 °C but for a lighter dose ($R_{sheet} \sim 90\,\Omega/sq$). Here, the lower sheet resistance at 1050 °C ($R_{sheet} = 27\,\Omega/sq$) of the BF_3-based emitters highlights the use of a too high dose, so for the study of the electrical quality of these emitters, that will follow in the next section, a lower implantation dose will be used.

4. IMPROVEMENTS OF DOSE/ANNEALING CONDITIONS

In this part, we study the impact of the implantation dose and annealing temperature variations on the electrical parameters (R_{sheet}, J_{0e}, and implied V_{oc}) of the BF_3-based emitters. We chose a lower BF_3 dose range, around a reference machine dose D_0 (range $D_0 \pm 2 \times 10^{15}$ at/cm^2). The textured wafers were symmetrically doped and submitted to standard thermal annealings around 1050–1075 °C, with different times for the temperature plateau. The substrates were then passivated with a SiO_2/SiN_x stack and finally fired in an infrared furnace. Electrical characterizations are shown in Figure 5. These new dose/annealing conditions give values of sheet resistance and J_{0e} closer to that obtained in our reference 90 Ω/sq BLII emitter [7]. The highest thermal budget always gives the best parameters.
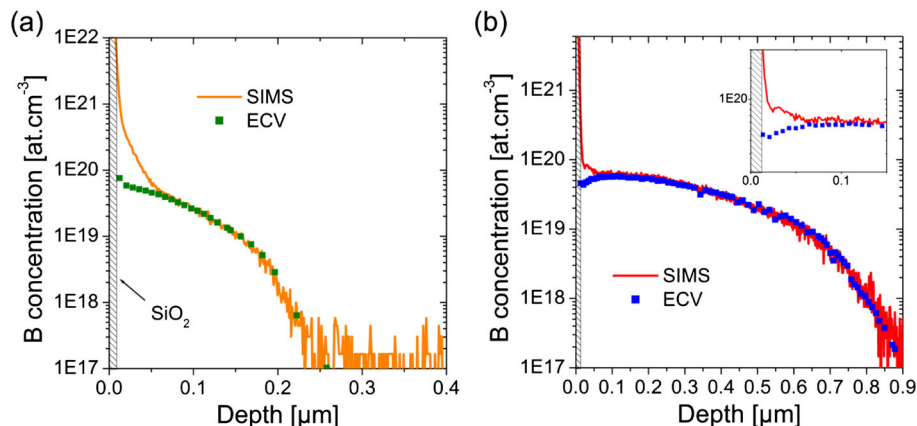
Figure 4. SIMS and ECV curves of heavily doped B emitters at two annealing conditions: (a) at 950 °C, giving 137 Ω/sq, and (b) at 1050 °C, giving 27 Ω/sq.
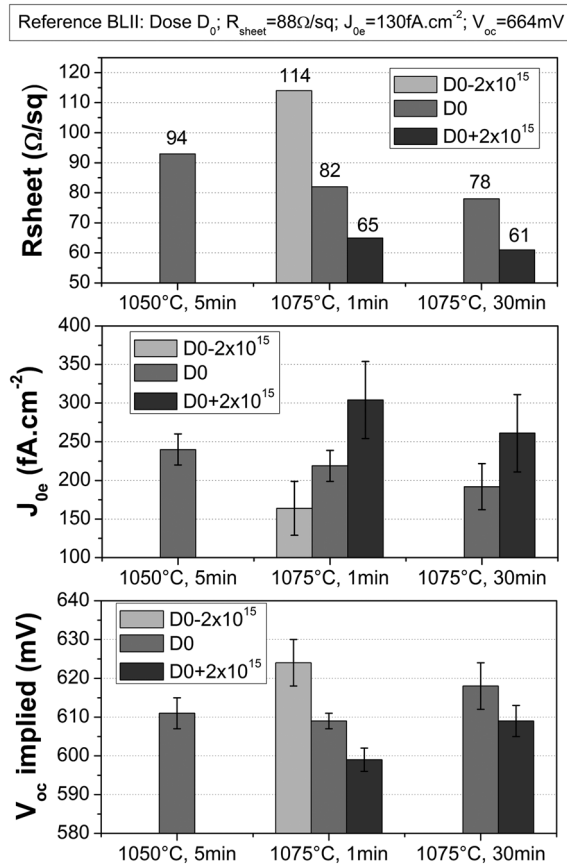
Figure 5. Electrical characterization of BF$_3$-based emitters for lighter implantation dose ranges (at/cm^2) around a reference dose D_0 and variable thermal budgets (SiO$_2$/SiN$_x$ passivation). The BLII reference is recalled in the top graph.

Notably, low saturation current densities validate the quality of the space charge zone and are an indication that the activation of BF$_3$ implants is complete, especially for the lowest dose (average J_{0e} ~160 fA/cm^2). The decrease of R_{sheet} and J_{0e} with the increase of the thermal budget (from 1 to 30 min at 1075 °C for instance) may be attributed to an increase of the carrier mobility μ_p resulting from a deeper

(less concentrated) profile, according to the well-known relation

$$R_{sheet} = \left[q \int_0^{x_j} \mu_p(x) N(x) dx \right]^{-1}$$

where x_j is the junction depth, N is the local active boron concentration, and μ_p is the hole mobility.

However, whereas J_{0e} values are quite low, implied V_{oc} remains surprisingly limited (below 630 mV) even for the lightly doped emitter. This is not the case for boron emitters performed by beamline (with pure B$^+$ ions). It is to be noted that other reported works on BF$_3$ plasma doping applied on float zone and ribbon silicon substrates, for similar dose ranges, also showed implied V_{oc} quite below 600 mV but with lower thermal budgets [28]. Two hypotheses (possibly combined) could explain the low V_{oc} phenomenon:

- A degradation of the bulk substrate lifetime (because of extra-contamination, enhanced during the high thermal annealing, or because of another physico-chemical phenomenon linked to the co-implantation of fluorine),
- A passivation issue at the surface (residual defects zone and/or bad interfacial oxide). This hypothesis should also normally impact the J_{0e} value.

In order to investigate the second hypothesis, fine SIMS measurements were done for boron and fluorine over the first 100-nm depth, on polished wafers that have been implanted and annealed with oxidation. On the as-implanted profiles, in Figure 6, we observe high concentrations of fluorine and boron, the B profile being slightly deeper. After annealing, there is the presence of a boron-rich oxide layer of a few nanometers thick. However, a remarkable effect is that we only detect fluorine inside the oxide with a relatively small concentration and not in the bulk substrate (or below the detection limit). Jeng *et al.* [29] experimentally showed that the SiO$_2$/Si interface clearly acts as a getter during thermal annealing and removes F from the interior of the sample. Thompson *et al.* [30] also stated that incorporation of ambient O$_2$ into the boron-doped silicon surface, during thermal steps, would enhance the out-diffusion of fluorine from the
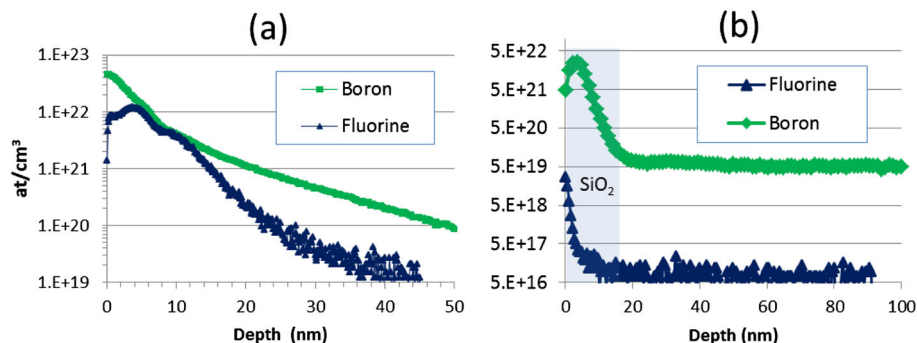
Figure 6. SIMS profiles of F and B (at/cm^3) just after implantation (a) and after annealing/oxidation (b), with a high machine dose 2.9×10^{16} at/cm^2 (polished wafer).

surface, while the actual driving force (chemical and/or electromotive effects) is not totally identified. Our SIMS observations are thus consistent with such references.

The boron-rich oxide may present insufficient passivation properties. However, such a layer may also exist in case of beamline emitters. These measurements let us think that, after the annealing, it is advisable to chemically treat the surface before oxidation/passivation, by etching the oxide and the superficial boron-rich silicon. We have tested this case and indeed observed an improvement of J_{0e} and V_{oc} (gain of 5 to 10 mV), but it is not sufficient to reach high voltage. Such a treatment is not necessary when we implant pure B^+ atoms (with a beamline). Another method could be to willingly grow a thick sacrificial oxide during the thermal annealing in order to largely consume the B-rich emitter surface and to remove it chemically afterwards [6]. A disadvantage, however, is that post-annealing chemical step prevents a direct passivation of the surface by growing a high-quality silicon oxide during the thermal activation (such an *in situ* passivation is very practical in a solar cell-manufacturing process). On the other hand, once the oxide is removed, we have the choice to make a better passivation like Al_2O_3 deposition [7] (a gain of ~10 mV can be expected, compared with SiO_2). After having clarified the passivation issue, one can wonder whether low V_{oc} are because of the immersion-plasma technique itself (with possible extra-contamination) or to the ion specie (with the subsequent physicochemical effects it implies). Indeed, as in the case of fluorine-based reactive ion etcher, BF_x^+ or F^+ ions might attack some parts

of the implantation chamber and incorporate metallic species into the wafers. We thus switched on beamline equipment and analyzed the differences observed when we implant pure B^+ ions or pure BF_x^+ ions exclusively.

5. A COMPARISON BETWEEN B^+ AND BF_2^+ IMPLANTATIONS

In a pulsed-plasma-immersion chamber, the gas precursor BF_3 is decomposed in different species like BF_2^+, BF^+, F^+, and B^+ but essentially BF_2^+ (more than 50% and most often between 85 and 95%) [14–16]. As a consequence, to study the impact of fluorine atoms on the emitter parameters, we implanted BF_2^+ ions with a (mass selective) beamline and compared it to our reference B^+ doping. It is to be noticed that BF_2^+ are heavier ions so that implantation energy should be increased (nearly 4.5 times more) to fit its profile with the as-implanted B^+ profile, but this leads to very high J_{0e} values (probably because of greater and deeper implantation damage, refer to [27]). Figure 7(a) shows CTRIM simulations comparing the reference boron profile and the BF_2^+ implanted ones at the same implantation energy (that of our reference boron emitter). As we will see, the final characteristic profiles after annealing become similar.

Double-side samples were implanted to obtain three different profiles noted (1), (2), and (3), whose implantation conditions are listed in Table I. As we use a microelectronics-class beamline tool in this section, the
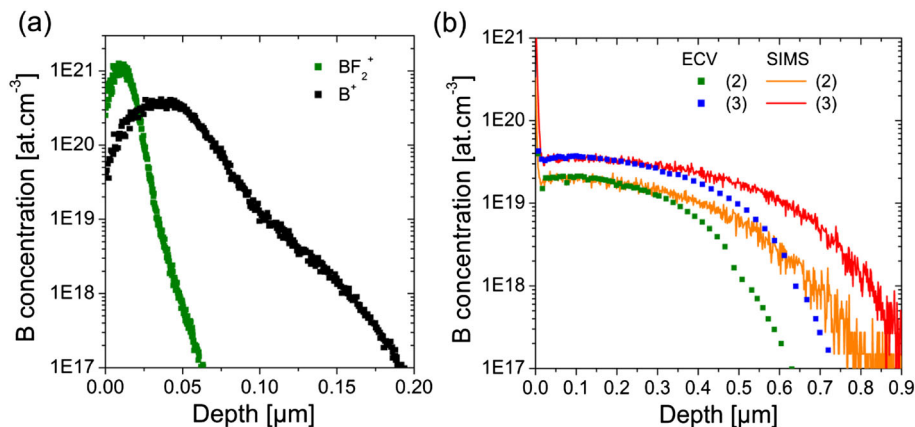
Figure 7. (a) Simulated profiles of as-implanted B^+ and BF_2^+ implants (before annealing) for same implantation energy and nominal dose D_0. (b) Comparison of ECV and SIMS measurements of BF_2^+ implants (emitters (2) and (3) listed in Table I) after annealing, showing complete activation.

Table I. Average electrical parameters of emitters based on B^+ or BF_2^+ ions, performed by beamline, for fixed implantation energy.

Emitter	Features	R_{sheet} (Ω/sq)	R_{sh} nonuniformity (%)	V_{oc} (mV)	J_{0e} (fA/cm^2)	τ bulk (µs)
(1)	B^+/dose D_0	97	3.1	663	122	244
(2)	BF_2^+/dose D_0	149	3.6	607	190	140
(3)	BF_2^+/~2.5× dose D_0	76	2.6	599	313	158

Samples are passivated by SiO_2/SiN_x stacks. τ is the effective lifetime of the bulk silicon measured after complete emitter etching (20 µm removed on each side) and SiN_x passivation (without subsequent firing).

real implanted dose is well controlled. They were annealed at 1050 °C and passivated with the usual SiO_2/SiN_x stack. All the samples were annealed together in the same furnace. The final doping profiles of BF_2^+ implants are displayed in Figure 7(b). ECV/SIMS curves confirm the complete activation of BF_2^+-based emitters (2) and (3) (the deviation here observed for great depths may be because of a calibration error or to the displacement of probed dopants by Cs + etching during SIMS experiment; this difference does not significantly modify the calculation of the active dose).

Final electrical parameters measured by QSS-PC are summed up in Table I. The sheet resistances of (1) and (2) emitters (same nominal dose) are clearly different. It is not linked to an activation degree or to a shallower doping profile but to a different final dose kept inside the substrate. The as-implanted BF_2^+ profile being more concentrated and closer to the surface, we may meet more boron exodiffusion during annealing (or more B removal during chemical cleaning if such a step is used just after implantation). An exodiffusion because of the co-implantation of F is another possible explanation, according to the scientific literature (refer to the Introduction section). Fluorine also seems to reduce the B cluster formation as the activation is total in the case of emitter (3) although the dose is much higher.

Now, if we consider the QSS-PC measurements, we see that BF_2-based emitters show acceptable J_{0e} values (space charge zone not impacted by fluorine implantation) but low implied V_{oc}, for both doses. We thus retrieve a behavior very similar to that obtained by PIII emitters. By comparison, our standard B^+ emitter works fine and allows us to preclude a possible implanter contamination. SIMS measurements (not shown) on the very first nanometers of emitters (2) and (3) also exhibit the same kind of surface profiles for fluorine and boron seen in Figure 6.

In order to verify if the V_{oc} drop comes from the bulk silicon or from post-implantation damage that would have not been completely annealed (like the EOR damage at the end of the recrystallized silicon region), the emitters have been completely etched (~20 μm on each side of the wafers) to measure the effective minority carrier lifetime τ_{eff} inside the core substrate (after cleaning and a SiN_x passivation without subsequent firing step). Results are

shown in Table I. We indeed observe a strong reduction of τ_{eff} in the case of BF_2^+-based samples, with a loss of around 100 μs compared with the substrates implanted with B^+ ions. The explanation for such lifetime degradation is not understood at the present time and needs further studies. We can suspect some extended (deep) defects after annealing and/or activation of recombination centers linked to the implantation of F atoms. It is also possible that BF_2^+-based emitters are more sensitive to even residual contamination compared with B^+ emitters during thermal steps.

6. ROLE OF FLUORINE: F⁺ IMPLANTS VERSUS AMORPHIZATION DEFECTS

To complete the previous section, other complementary tests were carried out with the beamline implanter in order to check the impact of *pure* fluorine ion implants and that of surface amorphization, on the effective minority carrier lifetime (QSS-PC measurement). We selectively implanted F^+ or Si^+ ions with adapted energy/doses corresponding to what we expect in as-implanted BF_2^+ profiles, through CTRIM simulations (not detailed here). The Si^+ case is expected to introduce only a defect quantity at the surface close to that of BF_2^+ implants (no dopant was then implanted).

As these tests were led with other n-type Cz wafers different from that of the previous section, new boron emitters were performed for a clear comparison (cases (a) and (b) in Table II). We have again applied a 1050 °C annealing for all the substrates, but the ramp-up before the maximum temperature plateau was modified: The starting/loading temperature is chosen lower than classically used in order to improve at best the epitaxial recrystallization and cure the implantation damage resulting from BF_2^+ implants and auto-implantation of Si^+ ions (but it is to the detriment of the total annealing time which is then increased). All the wafers were passivated with SiO_2/SiN_x stacks and fired. The results are resumed in Table II. The case (b) is directly correlated with the cases (d) (same fluorine dose implanted) and (f) (same amorphized layer thickness). The cases (e) and (g) are additional trials.

Once again, we check that BF_2^+ implants give J_{0e} values as good as B^+ ones (<100 fA/cm² here) but limited

Table II. IICharacterization of wafers selectively implanted with pure fluorine and silicon ions for energy/implantation doses close to that expected in BF_2^+ implants and performed by beamline.

Case	Implanted specie	Energy	Ion dose	R_{sheet} (Ω/sq)	V_{oc} (mV)	J_{0e} (fA/cm²)	Lifetime at 1Sun (μs)
(a)	B^+	E	D_0	88	661	78	
(b)	BF_2^+	E	D_0	139	630	90	
(c)	No implant		—				309
(d)	F^+	~E/2	2× D_0				159
(e)	F^+	~E/2	4× D_0				52
(f)	Si^+	E/2	1.25× D_0				204
(g)	Si^+	E/2	3× dose D_0				100

The starting temperature of the annealing ramp-up is here much lower than that of usual conditions to better cure the amorphization damage.

implied V_{oc}. When compared with the nonimplanted substrate (which has also seen the same thermal annealing), the F^+-implanted wafers show significantly lower minority carrier lifetimes (all the more that the fluorine dose increases, from case (d) to (e)). An auto-Si^+ implant may also deteriorate the crystalline quality of the surface (after annealing) but at a much lower level.

7. PERSPECTIVES

We have studied the making of solar-grade boron emitters by plasma immersion ion implantation from BF_3 gas, on large-area textured n-type Cz silicon substrates. The electrical activation of boron was performed by high thermal budget annealing. Complementary SIMS and ECV measurements allowed us to better analyze the dopant profiles and to testify on the good activation rates, even for strong doses. Fluorine may be beneficial to B activation. However, there are also unexpected drawbacks. The main observation reported in this work is that satisfactory J_{0e} values ($<200\,fA/cm^2$, with a SiO_2 passivation) can be obtained for sheet resistances below $100\,\Omega/sq$, but implied V_{oc} are systematically limited ($<630\,mV$), which is insufficient to make efficient solar cells ($660\,mV$ would be required). Pure B^+ implants do not exhibit such limitations. By judiciously comparing beamline and plasma immersion implantations, we think that low V_{oc} are not due to the PIII technique itself but, indirectly, to the co-implantation of fluorine inducing, after high thermal annealing, a significant degradation of the bulk lifetime. The reason for such degradation is not clearly established (deep defects after annealing and/or activation of recombination centers linked to the implantation of F atoms). Chemical treatment after annealing may improve a little bit the implied voltage (by removal of a boron-rich oxide for instance) and hydrogen passivation (e.g. forming gas anneal) could be a way to partly recover a good substrate lifetime, but it implies additional steps in the process flow that reduces the expected advantages of ion implantation as regards to process simplification (compared with gas diffusion).

The use of BF_3 gas precursor on plasma immersion or ion shower tool (without mass analyzer) may thus prevent attainment of high-quality solar cell precursors. The scarcity of probative works about BF_3 doping for solar cells, in the current scientific literature, may reflect this difficult issue (good J_{0e} values are not sufficient; repeatable high implied V_{oc} are also to be proven). Thus, this paper contributes to the advances on plasma doping and aims to shed light on possible obstacles that are of special interest for industrial companies designing implanters dedicated to high-throughput PV cell fabrication lines. It is worth noting that it is possible to overcome the bulk lifetime degradation by resorting to *laser* activation of BF_3 implants (instead of thermal annealing) as the laser only anneals the silicon surface (annealed depth of a few microns with a short-wavelength beam). This latter method shows positive results that will be presented at a later

time. At last, the gas precursor B_2H_6 is one of the possible alternatives for PIII doping, and studies are currently in progress.

REFERENCES

1. Chuduri SK. Simply implants. *Photon International* 2013; 48–53.
2. Le Perchec J, Lanterne A, Michel T, Gall S, Monna R, Torregrosa F, Roux L. 19.3% efficiency on p-type silicon solar cells by Pulsion plasma-immersion implantation. *Energy Procedia* 2013; **33**: 18–23.
3. Michel T, Le Perchec J, Lanterne A, Monna R, Torregrosa F, Ruox L, Commandré M. Phosphorus emitter engineering by plasma-immersion ion implantation for c-Si solar cells. *Solar Energy Materials and Solar Cells* 2015; **133**: 194–200.
4. Liu BW. The applications of plasma immersion ion implantation to crystalline silicon solar cells. *Energy Procedia* 2013; **38**: 289–296.
5. Shen ZN, Xia Y, Liu BW, Liu JH, Li CB, Li YT. Realization of conformal doping on multicrystalline silicon solar cells and black silicon solar cells by plasma immersion ion implantation. *Chinese Physics B* 2014; **23**: 118801.
6. Tao Y, Payne A, Upadhyaya VD, Rohatgi A. 20.7% efficient ion-implanted large area n-type front junction silicon solar cells with rear point contacts formed by laser opening and physical vapor deposition. *Progress in Photovoltaics: Research and Applications* 2014; **22**: 1030–1039.
7. Lanterne A, Le Perchec J, Coig M, Manuel S, Gall S, Tauzin A, Veschetti A. Understanding of the annealing temperature impact on ion implanted bifacial n-type solar cells to reach 20.3% efficiency. *Progress in Photovoltaics: Research and Applications* 2014. DOI:10.1002/pip.2574.
8. Larionova Y, Kiefer F, Lim B, Heinemeyer F, Peibst R, Brendel R, Emsley R, Dube C, Graff J. *Industrial ion implanted co-annealed and fully screen-printed bifacial n-PERT solar cells with low-doped back-surface fields, nPV-Workshop*. Konstanz, Germany, 2015.
9. Sheoran M, Emsley M, Howarth J, Graff J, Liu Y, Wu J, Wang X -S, Yang J, Li J, Zheng Y, Yan F, Wijekoon K. Fully implanted rear emitter n-type (FIRE) solar cells, Proceedings of the 29th European Photovoltaics and Solar Energy Conference 2014, Amsterdam, 867–870.
10. Wood R, Westbrook R, Jellison G. Excimer laser-processed oxide-passivated silicon solar cells of 19.5-percent efficiency. *IEEE Electron Dev Lett* 1987; **8**: 249–251.
11. Westbrook RD, Wood RF, Jellison GE. Glow discharge implanted, thermally annealed, oxide

passivated silicon solar cells of 19% efficiency. *Applied Physics Letters* 1987; **50**: 469.

12. http://www.intevac.com/wp-content/uploads/2014/06/Intevac-ENERGi-Technical-Papers.pdf 2014.

13. Nakamura K, Soga T, Murakami Y, Ohshita Y, N-type bifacial cell using simplified ion doping system, 40th IEEE PVSC Conference, 2014; 3649–3653.

14. Kaeppelin V, Carrere M, Torregrosa F, Mathieu G. Characterization of an industrial plasma immersion ion implantation reactor with a Langmuir probe and an energy-selective mass spectrometer. *Surface and Coatings Technology* 2002; **156**: 119–124.

15. Koo BW, Fang Z, Godet L, Radovanov SB, Cardinaud C, Cartry Gi, Grouillet A, Lenoble D. Plasma diagnostics in pulsed plasma doping (P2LAD) system. *IEEE Transactions on Plasma Science* 2004; **32**: 456–453.

16. Burenkov A, Hahn A, Spiegel Y, Etienne H, Torregrosa F. Simulation of BF3 plasma immersion ion implantation into silicon. *AIP Conference Proceedings* 2012; **1496**: 233.

17. Chang RD, Lin CH, Ho LW. Diffusion of boron near projected ranges of B and BF2 ions implanted in silicon. *Japanese Journal of Applied Physics* 2008; **47**: 8696.

18. Nieh CW, Chen LJ. Cross-sectional transmission electron microscope study of residual defects in BF_2^+-implanted (001) Si. *Journal of Applied Physics* 1986; **60**: 3114.

19. Minondo M. Préamorphisation du silicium par l'ion germanium et formation de jonctions ultra-fines P+/N, PhD Dissertation, Institut National Polytechnique de Grenoble 1994.

20. Shauly EN, Lachman-Shalem S. Activation improvement of ion implanted boron in silicon through fluorine co-implantation. *Journal of Vacuum Science and Technology B* 2004; **22**: 592.

21. Downey DF, Chow JW, Ishida E, Jones KS. Effect of fluorine on the diffusion of boron in ion implanted Si. *Applied Physics Letters* 1998; **73**: 1263–1265.

22. a) Mokhberi A. Griffin PB. Plummer JD, Paton E, McCoy S, Elliott K. A comparative study of dopant activation in boron, BF2, arsenic, and phosphorus implanted silicon. *IEEE Transactions on Electron Devices* 2002; **49**: 1183; b) Mokhberi A. Kasnavi R.

Griffin PB, Plummer JD. Fluorine interaction with point defects, boron, and arsenic in ion-implanted Si. *Applied Physics Letters* 2002; **80**: 3530.

23. Poon CH, See A. Effect of fluorine co-implant on boron diffusion in germanium preamorphized silicon during post-LSA rapid thermal annealing. *IEEE Transactions on Semiconductor Manufacturing* 2011; **24**: 333–337.

24. Lenoble D. Étude, réalisation et intégration de jonctions P+/N ultra-fines pour les technologies CMOS inférieures à 0,18 micromètre, PhD Thesis, Université de Toulouse, France, 2000.

25. Raghuwanshi M, Lanterne A, Le Perchec J, Pareige P, Cadel E, Gall S, Duguay S. Influence of boron clustering on the implanted emitter quality of silicon solar cells: an atom probe tomography study. *Progress in Photovoltaics: Research and Applications* 2015. DOI:10.1002/pip.2607.

26. Muller R, Benick J, Bateman N, Schön J, Reichel C, Richter A, Hermle M, Glunz SW. Evaluation of implantation annealing for highly-doped selective boron emitters suitable for screen-printed contacts. *Solar Energy Materials and Solar Cells* 2014; **120**: 431–435.

27. Krügener J, Peibst R, Bugiel E, Tetzlaff D, Kiefer F, Jestremski M, Brendel R, Osten HJ. Ion implantation of boric molecules for silicon solar cells. *Solar Energy Materials and Solar Cells* 2015; **142**: 12–17.

28. Derbouz K, Michel T, De Moro F, Spiegel Y, Torregrosa F, Belouet C, Slaoui A. Plasma immersion ion implantation of boron for ribbon silicon solar cells. *EPJ Photovoltaics* 2013; **4**: 45105.

29. Thompson K, Booske JH, Cooper RF, Gianchandani YB, Downey DF, Arevalo EA. Effect of microwave radiation on boron activation, 14th International Conference on Ion Implantation Technology. IEEE 2002; **544**.

30. Jeng SP, Ma TP, Canteri R, Anderle M, Rubloff GW. Anomalous diffusion of fluorine in silicon. *Applied Physics Letters* 1992; **61**: 1310–1312.